

A New Family of Bimetallic Framework Materials Showing Reversible Structural Transformations

Olha Sereda,[†] Fritz Stoeckli,[†] Helen Stoeckli-Evans,^{*,†} Oleg Dolomanov,[‡]
Yaroslav Filinchuk,[§] and Phil Pattison^{§,||}

Institute of Physics, University of Neuchâtel, rue Emile-Argand 11, CH-2009 Neuchâtel, Switzerland, Department of Chemistry, Durham University, Durham, DH1 3LE, U.K., Swiss Norwegian Beamlines at ESRF, BP-220, 38043 Grenoble, France, and Laboratoire de Crystallographie, École Polytechnique Fédérale de Lausanne, BSP, CH-1015 Lausanne, Switzerland

Received August 11, 2008; Revised Manuscript Received April 24, 2009

ABSTRACT: Three new bimetallic framework compounds, namely, $(([\text{Cd}_3(\text{tn})_4][\text{Co}(\text{CN})_6]_2) \cdot 5\text{H}_2\text{O})_\infty$ (**1**), $([\text{Cd}(\text{tn})]_3[\text{Cr}(\text{CN})_6]_2)_\infty$ (**2**), and $([\text{Cu}_2(\text{tn})_2][\text{Ru}(\text{CN})_6] \cdot 4\text{H}_2\text{O})_\infty$ (**3**), have been prepared in a very simple manner from the ligand 1,3-diaminopropane (tn), the hexacyanometalates $[\text{Co}(\text{CN})_6]^{3-}$, $[\text{Cr}(\text{CN})_6]^{3-}$ and $[\text{Ru}(\text{CN})_6]^{4-}$, and a metal(II) sulfate ($\text{M}^{\text{II}}\text{SO}_4$; $\text{M} = \text{Cd}^{2+}$, Cu^{2+}). They have been characterized by IR, X-ray diffraction, elemental analysis and immersion calorimetry. All three compounds have three-dimensional structures, with both the organic ligand and the cyanide groups acting as bridges. Compounds **1** and **3** have channels occupied by water molecules of crystallization. All three complexes are stable indefinitely when exposed to the air at room temperature; however, when compounds **1** and **3** are heated, they lose the water molecules of crystallization. The powder X-ray diffractograms of these dried and as yet unknown species are different from those of the original compounds. However, in a humid atmosphere both dried compounds readsorb water molecules and revert to the original structures, as shown by powder X-ray diffraction measurements. The adsorption properties of compounds **1** and **3** were studied using immersion calorimetry and in situ powder X-ray diffraction. In the case of compound **3** the heat of the structural transformation on rehydration was found to be ca. 19 ± 3 J/g.

Introduction

The domain of three-dimensional coordination polymers, or metal–organic frameworks (MOFs) as they are called today, is an intensely studied field of research, and the subject has been reviewed recently by various authors who are extremely active in this field.^{1–8} These compounds are of great interest owing to their potential applications in the areas of gas storage, gas separation, and heterogeneous catalysis.^{9–22} The majority of these compounds are homometallic and have been formed using organic carboxylates and transition metal salts.^{23–28} Some cyanide-bridged inorganic coordination polymers, prepared by assembling cyanometalate anions and transition metal complexes as building blocks, have also been found to have framework structures. The hexacyanometalates, $\text{M}^{\text{II}}(\text{CN})_6^{4-}$ and $\text{M}^{\text{III}}(\text{CN})_6^{3-}$, are good building blocks, and a number of multidimensional systems have been synthesized, some with interesting magnetic properties.^{29–34} Interest in the gas sorption properties of these compounds has increased in recent years.³⁵ However, only a small number of coordination polymers based on hexacyanometalates have been reported as being porous.^{36,37} Porous materials that show reversible phase transformations on loss and addition of solvent molecules have also been reported on recently.^{38–41}

We have focused our efforts on the synthesis of crystalline materials, since the attainment of well-defined structures is intimately linked to an understanding of the design, synthesis and properties of such materials. For example, using hexacyanochromate(III) it was possible to prepare bimetallic three-dimensional (3D) and chiral one-dimensional (1D) metal–organic

cyano-bridged materials which exhibit ferromagnetism.⁴² In another case, we have successfully prepared a bimetallic 3D metal–organic cyano-bridged framework material using 4,4'-bipyridine, tetracyanonickelate and copper sulfate.⁴³

Our interests are in the construction of materials, porous or not, in which such phase transformations take place.⁴⁴ Here we report on three new 3D metal–organic cyano-bridged frameworks, prepared in a very simple manner from the ligand 1,3-diaminopropane (tn), the hexacyanometalates $[\text{Co}(\text{CN})_6]^{3-}$, $[\text{Cr}(\text{CN})_6]^{3-}$ and $[\text{Ru}(\text{CN})_6]^{4-}$, and a metal(II) sulfate ($\text{M}^{\text{II}}\text{SO}_4$; $\text{M} = \text{Cd}^{2+}$, Cu^{2+}). In order to explore their potential adsorptive properties and to study the various phase transformations that take place, the techniques of immersion calorimetry and in situ powder X-ray diffraction have been used.

Experimental Section

Elemental analyses of carbon, hydrogen, and nitrogen were performed by the Microanalysis Service of the Laboratory of Pharmaceutical and Organical Propedeutical Chemistry at the University of Geneva (Geneva, Switzerland). Infrared spectra were measured using KBr pellets in the interval of $4000\text{--}40$ cm^{-1} using a Perkin-Elmer 1720X FT-IR spectrometer. Thermogravimetric (TG) analyses were carried out using a Mettler 4000 module. Samples were introduced in a closed aluminum oxide crucible and heated at rate 0.1 $^\circ\text{C min}^{-1}$ under nitrogen at atmospheric pressure. DSC measurements were done with a modified differential scanning calorimeter (Mettler Toledo DSC 822e), under N_2/He at a rate of 1 $^\circ\text{C/min}$. Immersion calorimetry experiments were carried out at 293 K on samples of $0.15\text{--}0.20$ g using a TIAN-CALVET type calorimeter.^{45,46} The outgassed sample was placed in the calorimetric cell which was then immersed into a water bath controlled by a thermoregulator system LUDA MS. The thermal flow was provided by 180 thermocouples of Cu/constantan connected to a nanovoltmeter PREMA 8017. The integral of the curve, $V = f(t)$, is proportional to the energy generated during the immersion process, $\Delta_i H$. The normal calibration of the calorimetry system was carried out with an electrical resistance. The accuracy varies between 4 and 5% depending on the absolute energy liberated in the process and on the amount of solid used.

* Corresponding author. Mailing address: Institut de Physique, Université de Neuchâtel, Rue Emile-Argand 11, CH-2009 Neuchâtel, Switzerland. E-mail: Helen.Stoeckli-Evans@unine.ch.

[†] University of Neuchâtel.

[‡] Durham University.

[§] Swiss Norwegian Beamlines at ESRF.

^{||} École Polytechnique Fédérale de Lausanne.

General Synthetic Procedures. Single crystals of compounds **1** and **2** were obtained only when the nonstoichiometric ratios of Cd(II) with M(III) cyanides were used. Use of the standard reaction ratios, 3:2 or 2:1, always resulted in the precipitation of insoluble powders.

(a) $([\text{Cd}_3(\text{tn})_4][\text{Co}(\text{CN})_6]_2 \cdot 5\text{H}_2\text{O})_\infty$ (**1**). To a solution of tn (0.220 mL, 2 mmol) and CdSO_4 (0.312 g, 1 mmol) in 30 mL of water, an aqueous solution of the $\text{K}_3[\text{Co}(\text{CN})_6]$ (0.332 g, 1 mmol) was added dropwise. The reaction mixture was stirred for 30 min, and then NaClO_4 (0.12 g, 1 mmol) was added to aid crystallization. After stirring and heating at 75 °C for a few minutes, the mixture was filtered. Light yellow square-shaped crystals of compound **1** appeared from the filtrate after some days, yield of 0.13 g (39%). Elemental analysis: found C, 25.05; H, 4.26; N, 24.50; $\text{C}_{24}\text{H}_{52}\text{N}_{20}\text{Cd}_3\text{Co}_2\text{O}_5$ requires C, 24.94; H, 4.53 N, 24.24%.

(b) $([\text{Cd}(\text{tn})_3][\text{Cr}(\text{CN})_6]_2)_\infty$ (**2**). To a solution of tn (0.220 mL, 2 mmol) and CdSO_4 (0.312 g, 1 mmol) in 30 mL of water, an aqueous solution of the $\text{K}_3[\text{Cr}(\text{CN})_6]$ (0.332 g, 1 mmol) was added dropwise. The reaction mixture was stirred for 30 min, and then NaClO_4 (0.12 g, 1 mmol) was added to aid crystallization. After stirring and heating at 75 °C for a few minutes, the mixture was filtered. Light yellow square-shaped crystals of compound **2** appeared from the filtrate after some days, yield of 0.14 g (42%). Elemental analysis: found: C, 27.10; H, 2.78; N, 26.31; $\text{C}_{24}\text{H}_{30}\text{Cd}_3\text{Cr}_2\text{N}_{20}$ requires C, 27.72; H, 2.91 N, 26.94%.

(c) $([\text{Cu}_2(\text{tn})_2][\text{Ru}(\text{CN})_6] \cdot 4\text{H}_2\text{O})_\infty$ (**3**). 1,3-Diaminopropane (1.0 mL, 12.0 mmol) was added under aerobic conditions to a concentrated aqueous solution (5 mL) of $\text{CuCl}_2 \cdot 2\text{H}_2\text{O}$ (2.05 g, 12.0 mmol) with continuous stirring, leading to the immediate precipitation of a green powder. An aqueous solution of Et_4NOH (0.52 g, 3.5 mmol) was then added to dissolve this precipitate, and the resulting dark-blue solution obtained was warmed (at ca. 60 °C for about 5 min) and then filtered in order to remove the small amount of precipitate that remained. An aqueous solution (20 mL) of $\text{K}_4[\text{Ru}(\text{CN})_6]$ (2.47 g, 6.0 mmol) was then added with continuous stirring. Slow concentration of the resulting solution at room temperature afforded prismatic green crystals of **3**, which were filtered off and air-dried, yield of 0.92 g (27.4%). Elemental analysis: found C, 23.39; H, 4.43; N, 22.86; $\text{C}_{12}\text{H}_{28}\text{N}_{10}\text{Cu}_2\text{Ru}_1\text{O}_4$ requires C, 23.84; H, 4.67; N, 23.17%.

X-ray Structural Determination. A yellow crystal of **1** ($0.5 \times 0.5 \times 0.5$), a yellow crystal of **2** ($0.50 \times 0.50 \times 0.50$) and a green crystal of **3** ($0.40 \times 0.30 \times 0.30$) were mounted on a Stoe IPDS II Image Plate Diffractometer System⁴⁷ equipped with a graphite-monochromator; Mo K α radiation ($\lambda = 0.71073$ Å). Data collections were performed at 173 K. The structures were solved by direct methods using the program SHELXS-97⁴⁸ and refined by full matrix least-squares on F^2 with SHELXL-97.⁴⁸ The tn ligand is disordered in **3**. The hydrogen atoms were included in calculated positions and treated as riding atoms. In general the water H atoms were refined with distance restraints. Further crystallographic and refinement details are given in Table 1.

Topological Analyses. The topological analyses of the 3D networks in compounds **1**, **2** and **3** were carried out using the program OLEX.⁴⁹ Full details are given in Table S1 of the Supporting Information.

X-ray Powder Diffraction. The powder samples were inserted in a glass capillary of 0.5 mm diameter. X-ray powder data were collected at room temperature on a computer controlled STOE STADI P focusing powder diffractometer^{50,51} equipped with a curved Ge(111) monochromator (Cu K α ; $\lambda = 1.54051$ Å). A STOE linear position sensitive detector was used. The compounds were measured in the range of $4^\circ \leq 2\theta \leq 90^\circ$ using a step width of 0.1° .

Variable Temperature Synchrotron Powder X-ray Diffraction. Variable temperature synchrotron powder diffraction measurements were carried out at the Swiss Norwegian Beamlines (BM01-A) using a MAR345 Image Plate detector, wavelength = 0.724312 Å, capillary to image plate distance 400 mm, exposure times 60 s, 20° oscillations about ϕ , 2θ limits 0 – 24° .

Results and Discussion

Crystal Structures. The crystal structure analysis of $([\text{Cd}_3(\text{tn})_4][\text{Co}(\text{CN})_6]_2 \cdot 5\text{H}_2\text{O})_\infty$ (**1**) revealed that it is a three-dimensional network with both tn and cyanide bridges. The asymmetric unit consists of half a $[\text{Co}(\text{CN})_6]^{3-}$ anion, one and a half $[\text{Cdt}]^{2+}$ cations, and 2.5 water molecules (Figure 1). Atom Cd2 is located on a 2-fold axis, while all the other atoms are at general positions.

Table 1. Crystallographic and Structure Refinement Data for **1**, **2** and **3**

	1	2	3
empirical formula	$\text{C}_{24}\text{H}_{50}\text{N}_{20}\text{O}_5\text{Cd}_3\text{Co}_2$	$\text{C}_{24}\text{H}_{40}\text{N}_{20}\text{Cd}_3\text{Cr}_2$	$\text{C}_{12}\text{H}_{28}\text{N}_{10}\text{O}_4\text{Cu}_2\text{Ru}$
formula mass	1153.90	1049.96	604.59
wavelength [Å]	0.71073	0.71073	0.71073
temperature [K]	173	173	173
crystal system	monoclinic	triclinic	monoclinic
space group	$C2/c$	$P\bar{1}$	$P2_1/n$
<i>a</i> (Å)	27.4141(15)	7.7143(7)	7.7882(10)
<i>b</i> (Å)	11.6135(6)	7.8308(7)	10.6489(17)
<i>c</i> (Å)	13.7184(9)	16.1529(14)	13.2933(16)
α (deg)	90	95.474(7)	90
β (deg)	105.136(7)	95.669(7)	90.70(1)
γ (deg)	90	91.569(7)	90
volume [Å ³]	4092.2(4)	965.91(15)	1102.4(3)
Z	4	1	2
calcd density [g/cm ³]	1.873	1.805	1.821
absorption coeff [mm ⁻¹]	2.387	2.215	2.627
measured reflns	21665	13543	8591
unique reflns/ R_{int}	5508/0.0184	5137/0.0239	2862/0.0275
obsd reflns [$I > 2\sigma(I)$]	5229	4981	2681
no. of params refined	261	251	182
R_1^a [$I > 2\sigma(I)$]	0.0153	0.0200	0.0365
wR_2^b [$I > 2\sigma(I)$]	0.0344	0.0531	0.0990

$$^a R_1 = \sum ||F_o| - |F_c|| / \sum |F_o|. \quad ^b wR_2 = [\sum w(F_o^2 - F_c^2)^2 / \sum wF_o^4]^{1/2}.$$

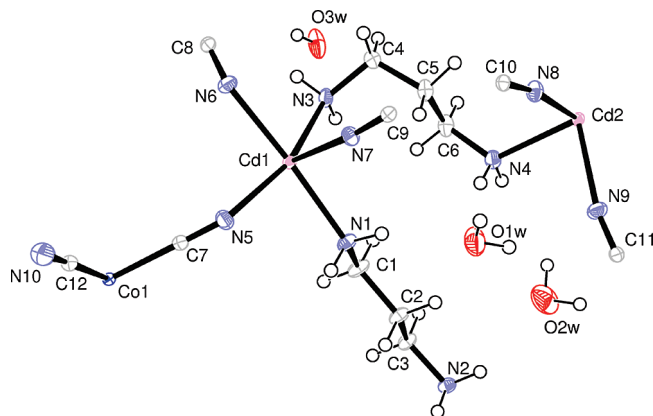


Figure 1. View of the asymmetric unit of **1**, showing the atom numbering scheme and displacement ellipsoids drawn at the 50% probability level.

Atom Cd1 is coordinated to three N atoms from tn ligands (one is bridging to Cd2 and the two others to Cd1) and three N atoms from the CN groups. Atom Cd2 also has an octahedral coordination, but is coordinated to only two N atoms from tn ligands (bridged to Cd1) and four from CN groups. The bond distances and angles in the diamine skeletons are in the expected range [average values: 1.483(2) Å for N–C, 1.518(2) Å for C–C, with bond angles of 123.02(11)° for Cd–N–C, and 114.05(14)° for C–C–C]; in good agreement with published work.⁵² The metal coordination environment of the hexacyanocobaltate(III) moiety is in good agreement with reported structures.^{53,54} The Cd–N bond lengths vary from 2.318(2) to 2.416(2) Å. Five of the six CN groups are bridging, while the sixth hydrogen bonds to water O3w located in the channel (Figure 2a). Finally, it is worth noting the unusual bridging coordination mode of the tn ligand, which leads to a Cd···Cd separation of 6.986(1) Å. The structure can be described as being formed of hexa-metallo-cycles consisting of only Cd atoms and tn ligands, which are connected via cyano bridges to form a three-dimensional (3D) network (Figure 2a, top).

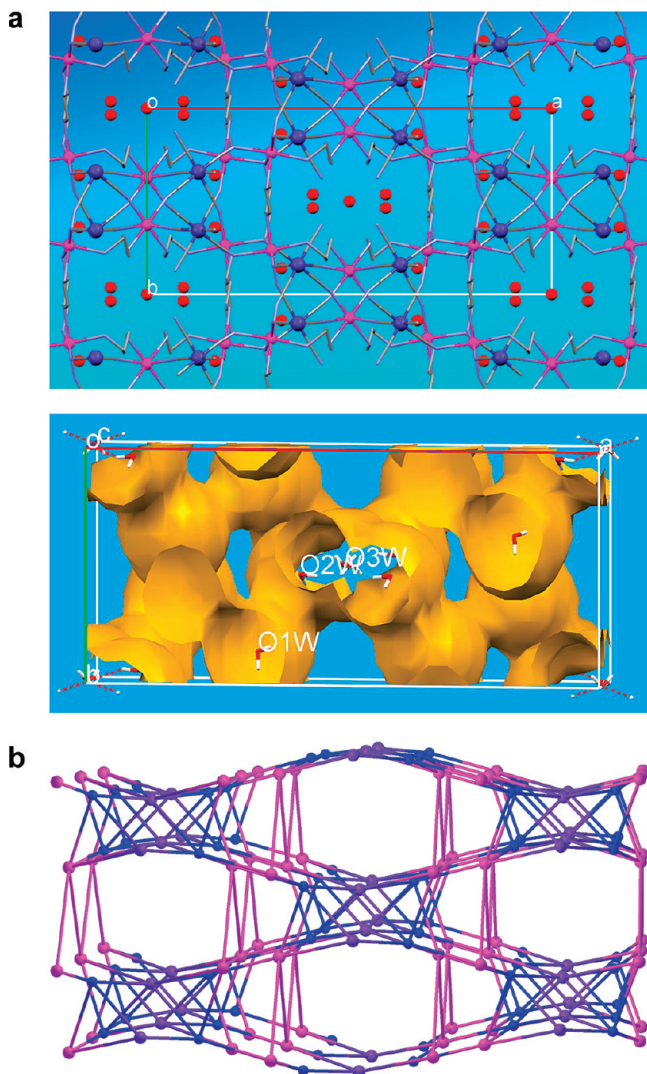


Figure 2. (a) Top: View down the *c* axis of the crystal packing in **1**. In the center can be seen the hexametallacycle, which is formed of Cd atoms (pink) bridged by tn ligands only. The water molecules in the cavities and channels are shown as red balls. The H atoms have been omitted for clarity. Bottom: A view down the *c* axis of the framework surface, showing water molecule O1W occupying a cavity, and water molecules O2W and O3W occupying the channels. (b) View of a fragment of the topological network of **1** along the crystallographic *c* direction. The Co1 atoms are shown in blue; Cd1, pink; Cd2, violet.

As shown in Figure 2a (bottom) water molecule O1W is situated in a small cavity, while water molecules O2W and O3W occupy channels (see also Figure S1 in the Supporting Information). They are hydrogen bonded to the terminal CN groups and the NH₂ groups of the tn ligands (Table S2 in the Supporting Information). The potential solvent volume of 484.4 Å³, occupied by the water molecules of crystallization, accounts for 11.8% of the volume of the unit cell (4092.2 Å³).⁵⁷

The topological analysis of **1** reveals a complex 3D extended framework structure, Figure 2b. The topological network has the (3¹4²5⁷6⁴7)₂(3¹4⁴5⁵)₂(3²4⁴5³6⁴) Schläfli^{55,56} symbol for the 6-connected Cd2, 5-connected Co1, and 6-connected Cd1 nodes, respectively. The framework forms large hexagonal channels propagating in the crystallographic *c* direction (Figure 2b), which are filled by water molecules (cf. Figures 2a and 2b).

The crystal structure analysis of ([Cd(tn)]₃[Cr(CN)₆]₂)_∞ (**2**) revealed that it is also a three-dimensional network with both

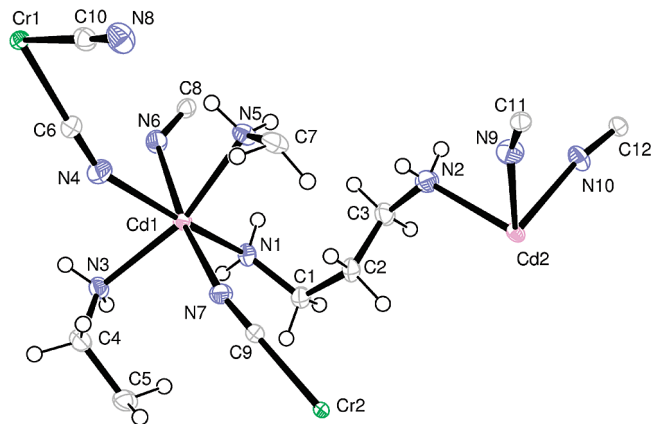


Figure 3. View of the asymmetric unit of **2**, showing the atom numbering scheme and displacement ellipsoids drawn at the 50% probability level.

tn and cyano bridges. The asymmetric unit consists of two half [Cr(CN)₆]³⁻ anions and 1.5 [Cd(tn)]²⁺ cations (Figure 3).

The Cr atoms of the hexacyanochromate(III) anions, Cr1 and Cr2, are located on inversion centers. Atom Cr1 coordinates to three adjacent [Cd1(tn)]²⁺ cations through four cyano nitrogens, while atom Cr2 coordinates to four adjacent [Cd2(tn)]²⁺ cations. Each Cr^{III} ion has almost regular octahedral coordination geometry. The Cr–C bond lengths are 0.16–0.18 Å longer than the Co–C bond lengths, as is usually observed.^{58,59} The Cd atoms have octahedral coordination geometries. Atom Cd1 sits at a general position, while atom Cd2 is located on an inversion center. The Cd–N(cyano) distances lie in the range 2.2878(16)–2.4511(16) Å, while the Cd–N(tn) distances average 2.385(15) Å, which is usual for six coordinated CdN₆.⁵²

Again the structure can be described as being formed of hexametallacycles consisting of only Cd1 atoms and tn ligands. They are connected via cyano bridges to form a three-dimensional network (Figure 4a). This time the cyano bridges involve penta-, tetra- and tris-metallacycles.

Topological analysis of compound **2** shows that the structure possesses a 3D extended framework constructed from four different nodes (Figure 4b) with overall (3¹4³5⁴6⁶7)₂(3²4⁶5⁴6³)-(3²4⁶5⁴6³)(4²5²6²) Schläfli symbol for the 6-connected Cd1, Cd2 and Cr2 and 4-connected Cr1 nodes, respectively. The environment of the topological nodes is shown in Figure S6 in the Supporting Information. The 6-connected Cd2 and Cr2 have the same Schläfli symbol.

Complex ([Cu₂(tn)₂][Ru(CN)₆]₂·4H₂O)_∞ (**3**) is isostructural with the iron(II) analogue,⁶⁰ and the structural features are similar to those of compounds **1** and **2**. The asymmetric unit of **3** consists of half a [Ru(CN)₆]⁴⁻ anion, a [Cu(tn)₂]²⁺ cation, and two water molecules of crystallization (Figure 5), atom Ru1 being situated on an inversion center.

The Ru–C and C–N bond distances and C–Ru–C angles are in good agreement with published values.^{61–64} The Cu^{II} ion is penta-coordinated, bonding to two nitrogen atoms of two equivalent tn ligands (N4, N5), and to three nitrogen atoms of the cyano groups (N1, N2 and N3). The N–Cu–N angles in the pseudo base deviate strongly from ideal trigonal-bipyramidal geometry (Figure 6). Such a distortion can be quantified using the τ parameter, as defined by Addison et al. ($\tau = 1$ for trigonal bipyramidal and 0 for square pyramidal).⁶⁵ The calculated value $\tau = 0.57$ indicates the extremely high degree of distortion of the coordination polyhedron.

In this structure, the tn ligand is again acting as a bridging ligand. The ruthenium ion, which has an almost regular

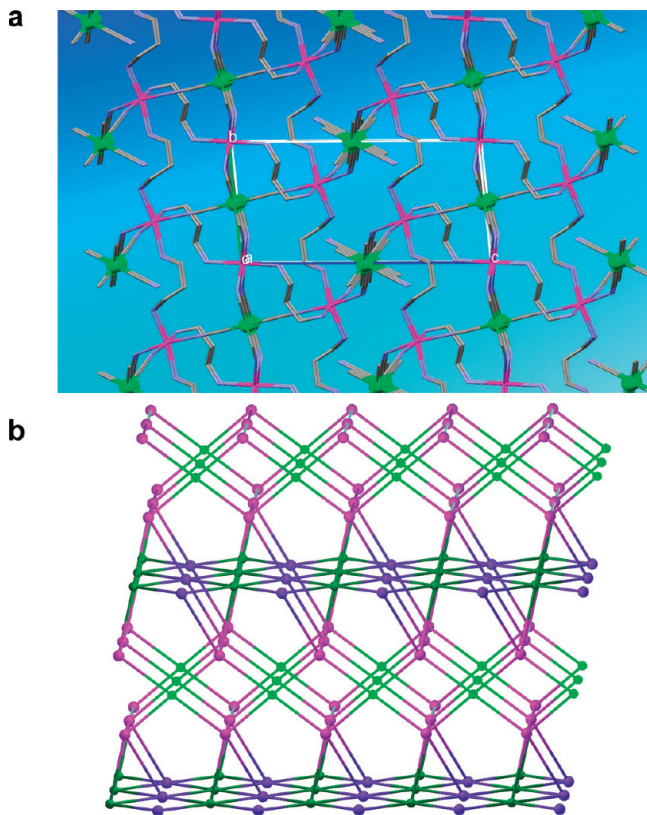


Figure 4. (a) View down the *a* axis of the crystal packing in compound **2** (Cd, pink; Cr, green). The H atoms have been omitted for clarity. (b) View along the crystallographic *b* direction of a fragment of the topological network for compound **2**. The Cr1 nodes are shown in light green; Cr2, dark green; Cd1, pink; Cd2, violet.

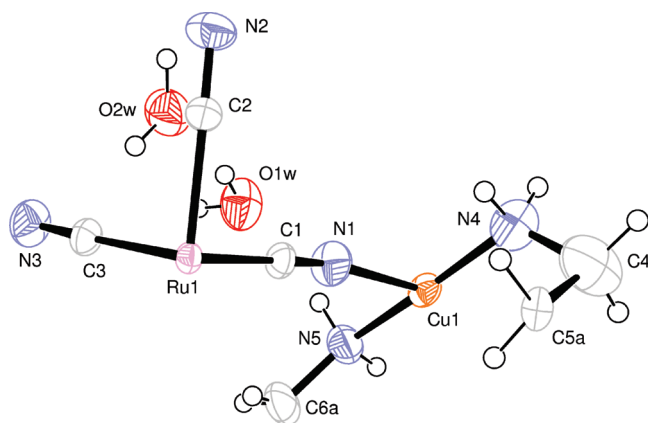


Figure 5. View of the asymmetric unit of the compound **3**, showing the atom numbering scheme and displacement ellipsoids drawn at the 50% probability level. The disordered atoms of the tn ligand have been omitted for clarity.

octahedral geometry, is linked to six copper(II) ions by six cyanide bridges, while the copper ion is linked to three equivalent $[\text{Ru}(\text{CN})_6]^{4-}$ anions. This leads to the formation of a three-dimensional arrangement in which the Ru—C≡N units are essentially linear, while the Cu—N≡C bond angles vary between 149.7(7) and 176.1(8)°.

As shown in Figure 6a (bottom) the water molecules occupy channels (see also Figure S2 in the Supporting Information). They are involved in hydrogen bonding with the terminal CN groups and the NH₂ groups of the tn ligands (Table S2 in the Supporting Information). The potential solvent volume of 174.3

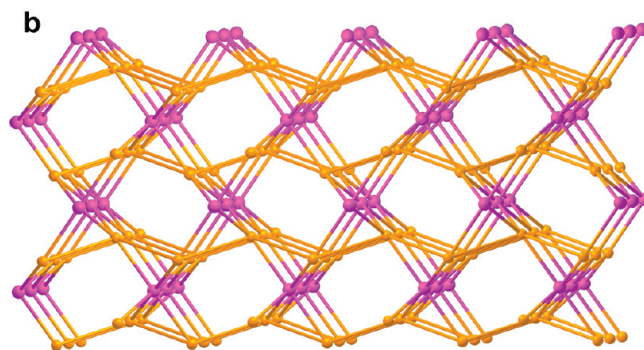
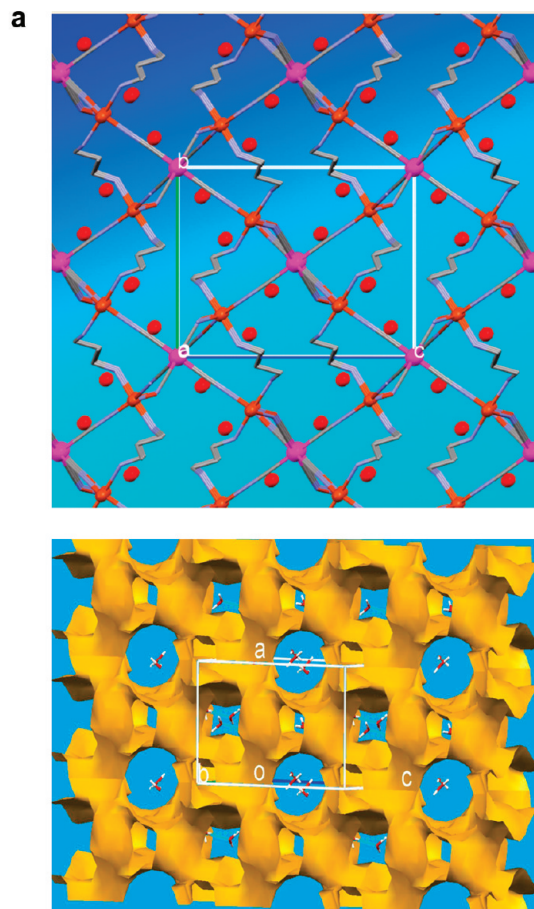


Figure 6. (a) Top: View along the *a* axis of the structure of compound **3** (Cu, orange; Ru, pink), showing the hexa-metalloccycles (The red balls represent water molecules. The H atoms have been omitted for clarity). Bottom: A view of the framework surface of compound **1** with the water molecules present in the channels. (b) View along the crystallographic *a* axis of a fragment of the topological network of compound **3**. The Ru nodes are shown in pink, Cu nodes in orange.

Å³, occupied by the water molecules of crystallization, accounts for 15.8% of the volume of the unit cell (1102.4 Å³).

This structure can be described as being formed of hexa-metalloccycles consisting of both tn and cyano bridges. They are further connected via cyano bridges to form a three-dimensional network (Figure 6a). This time the supplementary cyano bridges involve tetra- and tris-metalloccycles only.

The topological network of compound **3** (Figure 6b) consists of 6-connected Ru and 5-connected Cu nodes and has the $(3^2 4^1 5^3 6^4)_2 (3^2 4^2 5^6 6^2 7^3)$ Schläfli symbol for the Cu and Ru nodes, respectively (Figure S7 in the Supporting Information).

IR Analysis. The infrared spectra of compounds **1**, **2** and **3** exhibit the absorption bands expected for the tn ligand and the

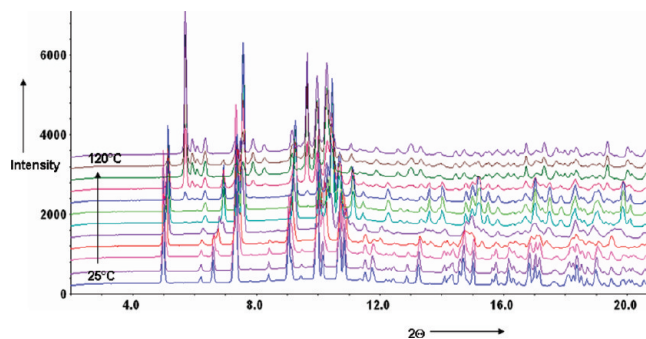
Table 2. Summary of the Immersion Calorimetry Experiments Performed on Compounds 1 and 3

sample	outgassing conditions	liquid	$-\Delta_i H$ (average) ± 3 , J/g
1	70 °C for 6 h	water	32.4
3	75 °C for 7 h	water	28.8
	20 °C for 7 h	water	47.8

hexacyanometalate counterions. The presence of the latter is clearly indicated by the strong absorption bands assignable to the $\nu(\text{C}\equiv\text{N})$ stretching vibrations in the range 2000–2200 cm^{-1} . Coordination of the CN ligand to a second metal ion through its nitrogen atom results in a displacement to higher wavelengths.⁶⁶ For **1** the shifts in the $\nu(\text{CN})$ stretching frequencies are from 2135 cm^{-1} in $\text{K}_3[\text{Co}(\text{CN})_6]$ ⁶⁷ to 2172 cm^{-1} , and for **2** the shifts are from 2130 cm^{-1} in $\text{K}_3[\text{Cr}(\text{CN})_6]$ ⁶⁷ to 2158 cm^{-1} . This clearly indicates the assembly of a $\text{Co}^{\text{III}}-\text{CN}-\text{Cu}^{\text{II}}$ bridge for **1** and a $\text{Cr}^{\text{III}}-\text{CN}-\text{Cu}^{\text{II}}$ bridge for **2**. The $\nu(\text{C}\equiv\text{N})$ stretching frequencies for **3** are found at 2095 cm^{-1} , which is in good agreement with the presence of $[\text{Ru}(\text{CN})_6]^{4-}$ units having at least one terminal CN ligand.^{32,63} The 1,3-diaminopropane ligand is also characterized by the presence in the IR spectrum of bands due to the $\nu(\text{NH})$ stretching vibrations of the NH_2 groups, in the 3150–3350 cm^{-1} region, and to the $\nu(\text{CH})$ stretching vibrations of the CH_2 groups, in the 2800–2980 cm^{-1} region.⁶⁸

Immersion Calorimetry and Heat of Structural Transformation. Immersion calorimetry is based on the determination of the enthalpy change occurring on immersing an outgassed nanoporous sample into a liquid; it is rapid to perform, sensitive and accurate.⁶⁹ The enthalpy change is related to the chemical and structural nature of the surface, and the enthalpy of immersion, $-\Delta_i H$, is equal to the integral of the net heat of adsorption.^{70,71} The studies carried out with compounds **1** and **3** showed that they have similar behavior for the adsorption of water (Table 2). In both cases, for the samples outgassed at 70 °C (**1**) and 75 °C (**3**), the heat of immersion is equivalent to the heat of filling of the nanopores plus the heat of the structural transformation.

It was possible to determine the heat of the structural transformation of compound **3** by outgassing a sample at 20 °C for 7 h under vacuum (10^{-3} Torr), giving a final weight loss of 12%. This procedure avoided any change in the structure of the compound on dehydration. The PXRD of this sample is indeed identical to that of the original compound **3** (Figure S3 in the Supporting Information). The heat of immersion of this sample gave the heat of filling of the nanopores alone, and was found to be higher than that for the sample outgassed at 75 °C (Table 2). The latter corresponds to the heat of filling of the nanopores plus the heat of the structural transformation. Hence, the difference in $-\Delta_i H$, i.e. ca. 19 ± 3 J/g, corresponds to the heat of transformation of the structure. To verify this, a sample of compound **3** outgassed at 20 °C was incubated at 25 °C for DSC measurement (heating from 25 to 120 °C at a rate of 10°min^{-1}). One endothermic effect of 21 J/g was observed. This value agrees well with the value expected from immersion calorimetry, that is, ca. 19 ± 3 J/g. The PXRD pattern of the sample after DSC corresponds to the PXRD pattern of **3** after TGA analysis (Figure S3 in the Supporting Information), indicating that on heating the change in the crystal structure had taken place. To the best of our knowledge this is the first time that the heat of a structural transformation has been demonstrated by two different methods. Unfortunately it was not possible to carry out the same analysis for compound **1**, as it already transforms to the dry form (weight loss of 7.85%) on outgassing at 20 °C.

**Figure 7.** In situ synchrotron powder X-ray diffraction (PXRD) patterns obtained on heating compound **3** from 25 to 120 °C.

Thermal Analyses, DSC and Powder X-ray Diffraction. The thermal stability of the water solvated compounds **1** and **3** was studied by thermogravimetric analysis (TGA) (Figure S4 in the Supporting Information) and differential scanning calorimetry (DSC) (Figure S5 in the Supporting Information). TGA for **1** indicates that the water molecules are completely removed at 130 °C in one step. There is a weight loss of 7.79% in the temperature range 25–125 °C, corresponding to the loss of five water molecules (theoretical value 7.78%). The TG curve for compound **3** clearly shows two steps in the weight loss. The first step is at ca. 60 °C with a weight loss of 6.10%, which correspond to two molecules of water (theoretical 5.9%). A final plateau is reached at ca. 85 °C with a weight loss of 6.04%. The total weight loss of 12.14% corresponds to the loss of four water molecules (theoretical value is 11.75%). The lability of the water molecules was shown by DSC measurements. The samples were incubated at 20 °C followed by heating at a rate of 10°min^{-1} to 100 °C. For compound **1** one endothermic effect of 113 J/g was observed at 95.4 °C, and for complex **3** one endothermic effect of 131 J/g was observed at 73.5 °C.

Some unique and intriguing phenomena were observed by in situ synchrotron powder X-ray diffraction (PXRD) measurements upon heating compound **3** (Figure 7). A capillary containing a powdered sample of **3** was slowly heated to 120 °C. There is a gradual change in the powder diffractogram from 25 to 65 °C, which is probably due to a slow loss of water molecules and shrinking of the unit cell. At 105 °C there is a definite change in the diffractogram, for example the intense peak at ca. 5° in 2θ , observable from 25 to 95 °C, has disappeared and a new intense peak appears at ca. 5.8° in 2θ . Finally, at 120 °C the diffractogram is identical to that of the sample recuperated after TGA, see Figure 9b. The structure of this new phase is unknown at present.

An interesting reversible structural transformation involving a crystalline, and not so highly crystalline state (after TG), was observed for compound **1** (Figure 8). The reversibility of this process was confirmed by PXRD measurements (Figures 8c and 8d). A capillary containing a powdered sample of **1** after TG (Figure 8b) was immersed into water for 90 min. The PXRD was then remeasured (Figure 8c), and it was found that the peak positions and intensities were identical with those observed for the single crystal of **1** (Figure 8a). Therefore, complex **1** exhibits “spongelike” molecular properties: it can easily take up water molecules and return to the original structure. It was possible to repeat this process a number of times without any loss of the crystallinity of **1** (Figure 8d).

The same “spongelike” behavior was also found for complex **3**. Figure 9a shows the PXRD pattern of **3** before heating. After heating to 120 °C under an inert atmosphere, all four water

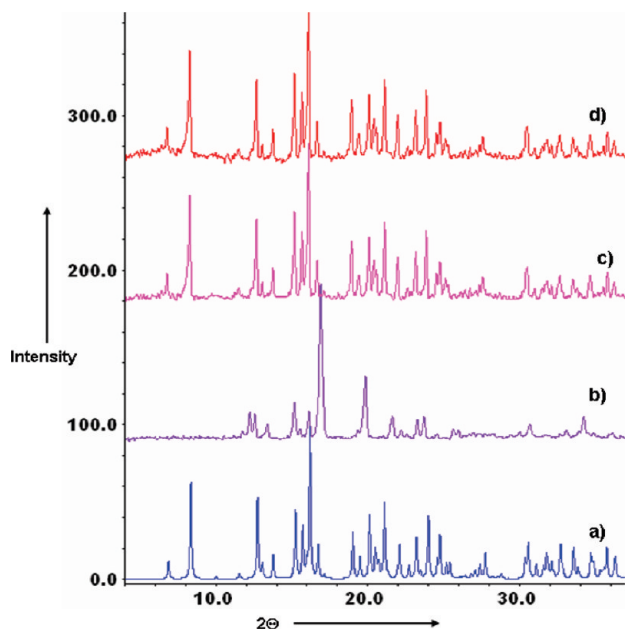


Figure 8. PXR D patterns for (a) a single-phase polycrystalline sample of **1**; (b) sample after being heated to 140 °C, at which point all five water molecules are lost; (c) sample from trace b after being placed in water for 90 min; and (d) sample after repeating the above procedure [a → b → c/a] at least three times.

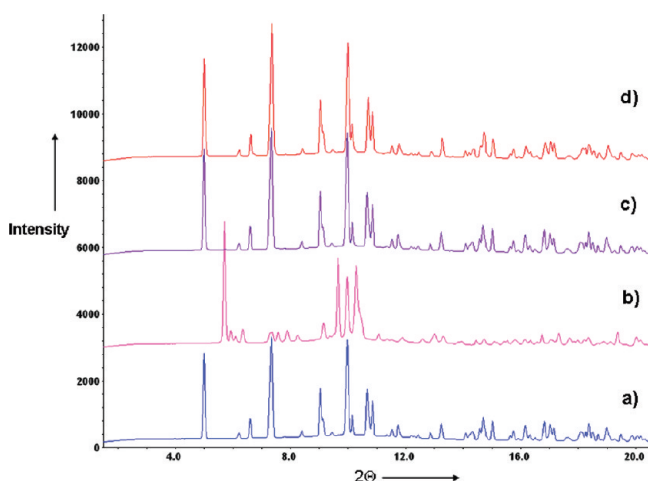


Figure 9. PXR D patterns for (a) a single-phase polycrystalline sample of **3**; (b) sample after being heated to 120 °C, at which point all four water molecules are lost and the sample color changed (from light-green to dark-green); (c) sample from trace b after being placed in water for 30 min (the color turned back to light-green); and (d) sample after repeating the above procedure [a → b → c/a] at least four times.

molecules were removed and the color of the sample changed from the original light-green to dark-green. The PXR D pattern taken at this point is shown in Figure 9b and clearly indicates that a change in the crystal structure had taken place.

In the IR spectrum of the dried sample there is no absorption band at $\sim 3537\text{ cm}^{-1}$, which corresponds to the vibration of the water O–H bonds. This is in full agreement with the observation of the loss of the water molecules after TGA. The results of the elemental analysis for this dried sample (found C, 27.39; H, 3.93; N, 26.86. $\text{C}_{12}\text{H}_{20}\text{N}_{10}\text{Cu}_2\text{Ru}_1$ requires C, 27.07; H, 3.79; N, 26.30%) confirmed the loss of all four water molecules. This dried sample was then placed in water for 30 min. The color turned from dark-green to the original light-green, and the

powder pattern taken at this stage (Figure 9c) is in excellent agreement with the original one, Figure 9a. The IR spectrum of this “wet” sample showed the reappearance of a strong band at 3537 cm^{-1} , indicative of the presence of water molecules in the structure. This reversible structural transformation process associated with a color change was repeated a number of times. Figure 9d is the PXR D pattern taken after the same procedure had been repeated four times on the original sample.

Conclusion

Three bimetallic cyano-bridged framework materials have been made in a very simple manner from inexpensive starting materials. Compounds $([\text{Cd}_3(\text{tn})_4][\text{Co}(\text{CN})_6]_2) \cdot 5\text{H}_2\text{O}$ (**1**), $([\text{Cd}(\text{tn})]_3[\text{Cr}(\text{CN})_6]_2) \cdot 5\text{H}_2\text{O}$ (**2**), and $([\text{Cu}_2(\text{tn})_2][\text{Ru}(\text{CN})_6]_2) \cdot 4\text{H}_2\text{O}$ (**3**) have been synthesized using a common organic ligand, 1,3-diaminopropane, a potassium hexacyanometalate and a transition metal salt. These new materials have been fully characterized and shown to have 3D framework structures. Compounds **1** and **3** have cavities and channels occupied by water molecules of crystallization and show “spongelike” dynamic behavior triggered by guest removal and inclusion. It was shown by immersion calorimetry and in situ powder X-ray diffraction that the dehydration/rehydration processes, which involve changes in the structures of **1** and **3**, are reversible. The heat of the structural transformation on rehydration of **3** was found to be $\text{ca. } 19 \pm 3\text{ J/g}$. Work is in progress to understand how these structural transformations take place. Further gas/solid and liquid/solid adsorption studies, and in situ X-ray diffraction studies, involving both water and other solvents, are currently in progress.

Acknowledgment. This work was financed by the Swiss National Science Foundation (Grant No. 20-111738). We are also grateful to the Swiss-Norwegian Beamlines for the provision of synchrotron beam time.

Supporting Information Available: Additional figures and tables including crystal packing in **1** and **3**, PXR D for **3**, TG and DSC curves of **1** and **3**, topological analysis for **1–3**, and hydrogen bonding in **1** and **3**. This material is available free of charge via the Internet at <http://pubs.acs.org>.

References

- Batten, S. R.; Neville, S. M.; Turner, D. *Coordination Polymers: Design, Analysis and Application*; Royal Society of Chemistry: 2009; Vol. 1.
- Tranchemontagne, D. J.; Ni, Z.; O’Keeffe, M.; Yaghi, O. M. *Angew. Chem., Int. Ed.* **2008**, *47* (28), 5136.
- Ferey, G. *Stud. Surf. Sci. Catal.* **2007**, *170A*, 66.
- Maji, T. K.; Kitagawa, S. *Pure Appl. Chem.* **2007**, *79* (12), 2155.
- Kubota, Y.; Takata, M.; Kobayashi, T. C.; Kitagawa, S. *Coord. Chem. Rev.* **2007**, *251* (21–24), 2510.
- Serre, C.; Mellot-Draznieks, C.; Surlé, S.; Audebrand, N.; Filinchuk, Y.; Férey, G. *Science* **2007**, 1828.
- Rowse, J. L. C.; Yaghi, O. M. *Microporous Mesoporous Mater.* **2004**, *73* (1–2), 3–14.
- Rosi, N. L.; Eddaoudi, M.; Kim, J.; O’Keeffe, M.; Yaghi, O. M. *CrystEngComm* **2002**, *4*, 401.
- Kitagawa, S.; Kitaura, R.; Noro, S.-I. *Angew. Chem.* **2004**, *116*, 2388.
- Moulton, B.; Zaworotko, M. *Chem. Rev.* **2001**, *101*, 1629.
- Eddaoudi, M.; Moler, D. B.; Li, H.; Chen, B.; Reineke, T. M.; O’Keeffe, M.; Yaghi, O. M. *Acc. Chem. Res.* **2001**, *34*, 319.
- Fujita, M.; Know, Y. J.; Washizu, S.; Ogura, K. *J. Am. Chem. Soc.* **1994**, *116*, 1151.
- Millange, F.; Serre, C.; Guillou, N.; Férey, G.; Walton, R. I. *Angew. Chem., Int. Ed.* **2008**, *47*, 4100.
- Ferey, G. *Chem. Soc. Rev.* **2008**, *37* (1), 191.
- Maji, T. K.; Kitagawa, S. *Pure Appl. Chem.* **2007**, *79* (12), 2155.
- Latroche, M.; Suble, S.; Serre, C.; Mellot-Draznieks, C.; Llewellyn, P. L.; Lee, J.-H.; Chang, J.-S.; Jung, S. H.; Férey, G. *Angew. Chem., Int. Ed.* **2006**, *45*, 8227.

- (17) Llewellyn, P. L.; Maurin, G.; Devic, T.; Loera-Serna, S.; Rosenbach, N.; Serre, C.; Bourrelly, S.; Horcajada, P.; Filinchuk, Y.; Férey, G. *J. Am. Chem. Soc.* **2008**, *130*, 12808.
- (18) Banerjee, R.; Phan, A.; Wang, B.; Knobler, C.; Furukawa, H.; O’Keeffe, M.; Yaghi, O. M. *Science* **2008**, *319* (5865), 939.
- (19) Xue, M.; Zhu, G.; Ding, H.; Wu, L.; Zhao, X.; Jin, Z.; Qiu, S. *Cryst. Growth Des.* **2009**, *9* (3), 1481.
- (20) Galli, S.; Masciocchi, N.; Tagliabue, G.; Sironi, A.; Navarro, J. A. R.; Salas, J. M.; Mendez-Linan, L.; Domingo, M.; Perez-Mendoza, M.; Barea, E. *Chem.—Eur. J.* **2008**, *14*, 9890.
- (21) Mueller U. Schubert, M. M. Yaghi, O. M. *Handbook of Heterogeneous Catalysis*, 2nd Ed.; Wiley-VCH Verlag GmbH & Co. KGaA: Weinheim, Germany, 2008; Vol. 1, pp 247–262.
- (22) Rowsell, J. L.; Yaghi, O. M. *Angew. Chem., Int. Ed.* **2004**, *44* (30), 4670.
- (23) Choi, J. Y.; Jeo Kim, J.; Furukawa, H.; Chae, H. K. *Chem. Lett.* **2006**, *35*, 1054.
- (24) Li, H.; Eddaoudi, M.; O’Keeffe, M.; Yaghi, O. M. *Nature* **1999**, *402*, 276.
- (25) Yaghi, O. M.; O’Keeffe, M.; Ockwig, N. W.; Chae, H. K.; Eddaoudi, M.; Kim, J. *Nature* **2003**, *423*, 705.
- (26) Chae, H. K.; Siberio-Perez, D. Y.; Kim, J.; Go, Y.-B.; Eddaoudi, M.; Matzger, A. J.; O’Keeffe, M.; Yaghi, O. M. *Nature* **2004**, *427*, 523.
- (27) Dybtsev, D. N.; Chun, H.; Yoon, S. H.; Kim, D.; Kim, K. *J. Am. Chem. Soc.* **2004**, *126*, 32.
- (28) Serre, C.; Surble, S.; Mellot-Draznieks, C.; Filinchuk, Y.; Férey, G. *Dalton Trans.* **2008**, 5462.
- (29) Ohba, M.; Fukita, N.; Okawa, H. *J. Am. Chem. Soc.* **1997**, *119*, 1011.
- (30) Miyasaka, H.; Matsumoto, N.; Okawa, H.; Re, N.; Gallo, E.; Floriani, C. *J. Am. Chem. Soc.* **1996**, *118*, 981.
- (31) Coronado, E.; Gimenez-Saiz, C.; Martinez-Agudo, J. M.; Nuez, A.; Romero, F. M.; Stoeckli-Evans, H. *Polyhedron* **2003**, *22*, 2435.
- (32) Shek, I. P.-Y.; Yeung, W.-F.; Lau, T.-C.; Zhang, J.; Gao, S.; Szeto, L.; Wong, W.-T. *Eur. J. Inorg. Chem.* **2005**, 364.
- (33) Zhoua, H.; Chena, Y.-Y.; Yuana, A.-H.; Shenb, X.-P. *Inorg. Chem. Commun.* **2008**, *11*, 363.
- (34) Agustí, G.; Muñoz, M. C.; Gaspar, A. B.; Real, J. A. *Inorg. Chem.* **2009**, *48* (8), 3371.
- (35) Beauvais, L. G.; Long, J. R. *J. Am. Chem. Soc.* **2002**, *124*, 12096.
- (36) Pretsch, T.; Chapman, K. W.; Halder, G. J.; Kepert, C. J. *Chem. Commun.* **2006**, 1857.
- (37) Chapman, K. W.; Chupas, P. J.; Kepert, C. J. *J. Am. Chem. Soc.* **2006**, *128*, 7009.
- (38) Galli, S.; Masciocchi, N.; Tagliabue, G.; Sironi, A.; Navarro, J. A. R.; Salas, J. M.; Mendez-Linan, L.; Domingo, M.; Perez-Mendoza, M.; Barea, E. *Chem.—Eur. J.* **2008**, *14*, 9890.
- (39) Bauer, S.; Marrot, J.; Devic, T.; Férey, G.; Stock, N. *Inorg. Chem.* **2007**, *46*, 9998.
- (40) Maji, T. K.; Mostafa, G.; Matsuda, R.; Kitagawa, S. *J. Am. Chem. Soc.* **2005**, *127* (49), 17152.
- (41) Iremonger, S. S.; Southon, P. D.; Kepert, C. J. *Dalton Trans.* **2008**, *44*, 6103.
- (42) Sereda, O.; Ribas, J.; Stoeckli-Evans, H. *Inorg. Chem.* **2008**, *47* (12), 5107.
- (43) Sereda, O.; Stoeckli-Evans, H. *Acta Crystallogr.* **2008**, *C64* (6), m221.
- (44) Sereda, O.; Neels, A.; Stoeckli, F.; Stoeckli-Evans, H.; Filinchuk, Y. *Cryst. Growth Des.* **2008**, *8* (7), 2307.
- (45) Bansal, R. C. Donnet, J. B. Stoeckli, F. *Active Carbon*; Marcel Dekker: New York, 1988.
- (46) Stoeckli, F.; Hugi-Cleary, D.; Centeno, T. A. *J. Eur. Ceram. Soc.* **1998**, *18*, 1177.
- (47) Stoe & Cie. *IPDS-2 Software*; Stoe & Cie GmbH: Darmstadt, Germany, 2006.
- (48) Sheldrick, G. M. *Acta Crystallogr.* **2008**, *A64*, 112.
- (49) Dolomanov, O. V.; Blake, A. J.; Champness, N. R.; Schröder, M. *J. Appl. Crystallogr.* **2003**, *36*, 1283.
- (50) Wolfel, E. R. *J. Appl. Crystallogr.* **1981**, *14*, 291.
- (51) Wolfel, E. R. *J. Appl. Crystallogr.* **1983**, *16*, 341.
- (52) Yuge, H.; Mamada, A.; Asai, M.; Nishikiori, S.; Iwamoto, T. *Dalton Trans.* **1995**, 3195.
- (53) Marvaud, V.; Decroix, C.; Sculler, A.; Guyard-Duhayon, C.; Vaissermann, J.; Gonnet, F.; Verdaguer, M. *Chem.—Eur. J.* **2003**, *9*, 1677.
- (54) Eckhardt, R.; Hanika-Heidl, H.; Fischer, R. D. *Chem.—Eur. J.* **2003**, *9*, 1795.
- (55) Wells, A. F. *Three Dimensional Nets and Polyhedra*; John Wiley & Sons: New York, 1977.
- (56) Wells, A. F. *Further Studies of Three-Dimensional Nets*; ACA Monograph No. 8; American Crystallographic Association: 1979.
- (57) Spek, A. L. *J. Appl. Crystallogr.* **2003**, *36*, 7.
- (58) Kohn, J. A.; Townes, W. D. *Acta Crystallogr.* **1961**, *14*, 617.
- (59) Jagner, S.; Ljungstrom, E.; Vannerberg, N.-G. *Acta Chem. Scand., Ser. A* **1974**, *28*, 623.
- (60) Triki, S.; Sala-Pala, J.; Thétiot, F.; Gomes-Garcia, C. J.; Daran, J.-C. *Eur. J. Inorg. Chem.* **2006**, 185.
- (61) Mullica, D. F.; Hayward, P. K.; Sappenfield, E. L. *Inorg. Chim. Acta* **1995**, *237*, 111.
- (62) Mullica, D. F.; Hayward, P. K.; Sappenfield, E. L. *Inorg. Chim. Acta* **1996**, *253*, 97.
- (63) Rüegg, M.; Ludi, A.; Rieder, K. *Inorg. Chem.* **1971**, *10*, 1773.
- (64) Mullica, D. F.; Sappenfield, E. L. *Inorg. Chim. Acta* **1997**, *258*, 101.
- (65) Addison, A. W.; Rao, T. N.; Reedijk, J.; van Rijn, J.; Verschoor, G. *J. Chem. Soc., Dalton Trans.* **1984**, *7*, 1349.
- (66) Nakamoto, K. *Infrared and Raman Spectra of Inorganic and coordination Compounds*, 3rd ed.; Wiley: New York, 1978.
- (67) Uehara, A.; Terabe, S.; Tsuchiya, R. *Inorg. Chem.* **1983**, *22*, 2864.
- (68) Mondal, N.; Saha, M. K.; Bag, B.; Mitra, S.; Gramlich, V.; Ribas, J.; Fallah, M. S. E. *J. Chem. Soc., Dalton Trans.* **2000**, 1601.
- (69) IUPAC Recommendations. *Pure Appl. Chem.*, *66*, **1994**.
- (70) Stoeckli, F. *Adsorpt. Sci. Technol.* **1993**, *11*, 3.
- (71) Stoeckli, F.; Hugi-Cleary, D.; Centeno, T. A. *J. Eur. Ceram. Soc.* **1998**, *18*, 1177.

CG800883X